Heavy Ion Test Report for the AD9257-EP Analog-to-Digital Converter

Dakai Chen[1], Hak Kim[2], Ali Feizi[3],
Ted Wilcox[2], Christina Seidleck[2], and Anthony Phan[2]

1. NASA Goddard Space Flight Center, Code 561, Greenbelt, MD 20771
2. ASRC Space & Defense, c.o. NASA Goddard Space Flight Center
3. A.K. Aerospace Technology Corporation, c.o. NASA Goddard Space Flight Center

Test Date: June 27-28 and August 10, 2016

I. Introduction

The purpose of this test campaign is to determine the heavy ion-induced single-event effect (SEE) susceptibility of the AD9257-EP from Analog Devices.

II. Test Goals

The primary goals of the heavy ion test are summarized below.

1. Determine the single-event latchup (SEL) susceptibility at room temperature
    a. Determine SEL linear energy transfer (LET) threshold
    b. Determine characteristics of SEL, including whether the latchup is immediately destructive, or stable in a latched state
2. Determine single-event upset (SEU) and single-event functional interrupt (SEFI) LET threshold and saturating cross section
    c. Obtain SEU waveforms for applicable operating condition
    d. Derive SEU cross section for rate prediction
    e. Collect sufficient number of SEFI events for rate prediction given time restraints

III. Device Under Test

The AD9257-EP is an octal, 14-bit, low power, analog-to-digital converter (ADC). The product is capable of operating at a conversion rate up to 65 MSPS. The ADC requires a single 1.8-V power supply and LVPECL-/ CMOS-/LVDS-compatible sample rate clock for full performance operation. The device is built on a commercial 180-nm CMOS process. Therefore it is potentially susceptible to single-event latchup (SEL).

Figure 1 shows a functional block diagram of the device. Table I shows the basic part and test details. Detailed device parameters and functional descriptions can be found in the datasheet.

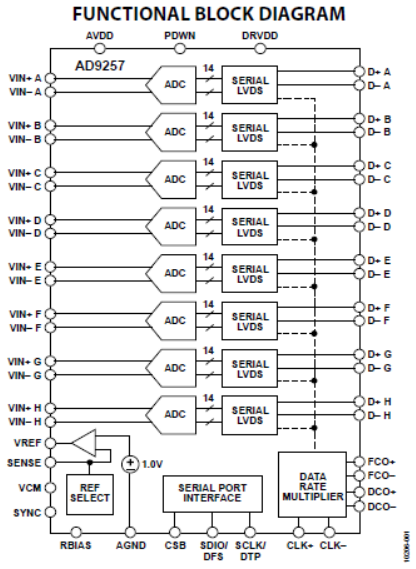

Figure 1. Schematic block diagram.

Table I: Part and test information.

Generic Part Number:	AD9257
Full Part Number	AD9257TCPZ-65-EP
Manufacturer:	Analog Devices
Lot Date Code (LDC):	1450
Quantity Tested:	3
Serial Numbers of Radiation Samples:	2, 6, 7
Part Function:	Analog-Digital Converter
Part Technology:	180 nm CMOS
Case Markings:	AD9257TCPZ-65-EP
Package Style:	64-Lead Lead Frame Chip Scale Package (LFCSP_VQ)
Test Equipment:	AD9257-65EBZ evaluation board HSC-ADC-EVALCZ controller board PC

IV. Test Facility

The heavy-ion beam testing was carried out at the Lawrence Berkeley National Laboratory (LBNL) Berkeley Accelerator Space Effects (BASE) Facility. The facility utilizes an 88-inch cyclotron to accelerate a cocktail of ions. The testing was performed in vacuum.

Facility: Lawrence Berkeley National Laboratory
Cocktail: 10 MeV/amu
Flux: Typically 1×10^3 to 1×10^5 ions/cm^2·s
Fluence: Typically 1×10^6 to 1×10^7 ions/cm^2 per run
Ions: Shown below in Table II

Table II
Heavy-ion specie, linear energy transfer (LET) value, range, and energy.

Ion	Initial LET in air (MeV·cm^2/mg)	Range in Si (µm)	Energy (MeV)
B	0.9	306	108
Ne	3.5	175	216
Si	6.1	142	292
Ar	9.7	130	400
Cu	21.2	108	659
Xe	49.3	148	1232
Au	85.8	90	1956

V. Test Method

A. Test Setup

The device under test (DUT) was configured as a part of the evaluation platform consisting of the AD9257-65EBZ evaluation card and the HSC-ADC-EVALCZ controller board. The evaluation platform features serial peripheral interface (SPI) communication for setup and control, choice of external or on-board oscillator, on-board regulator, and manufacturer-provided Visual Analog and SPI controller software interfaces.

The default test setup uses the Analog Devices high speed converter controller board (HSC-ADC-EVALCZ) for data capture. The serial LVDS outputs from the ADC are routed to Connector P1302 using 100 Ω differential traces. The capture program allows the user to record a continuous data stream. The program was not designed record SEU only. We created a post processing program which processes the output log from the deep capture and save the events that meet the trigger conditions, qualifying as single-event upsets (SEU). To allow for extended capture time, we modified the controller board by installing a larger capacity SRAM (GS8342T36BGD-250 from GSI Technology). The updated boards allow the deep capture program to record 4 MB of data.

Additionally, board modification was done to accommodate an external power supply. This allows visibility and current limiting capability of the supply current during single-event latchup testing. Figure 2 shows a schematic of a typical measurement setup, consisting of the AD9257-65EBZ evaluation card and HSC-ADC-EVALCZ controller board.

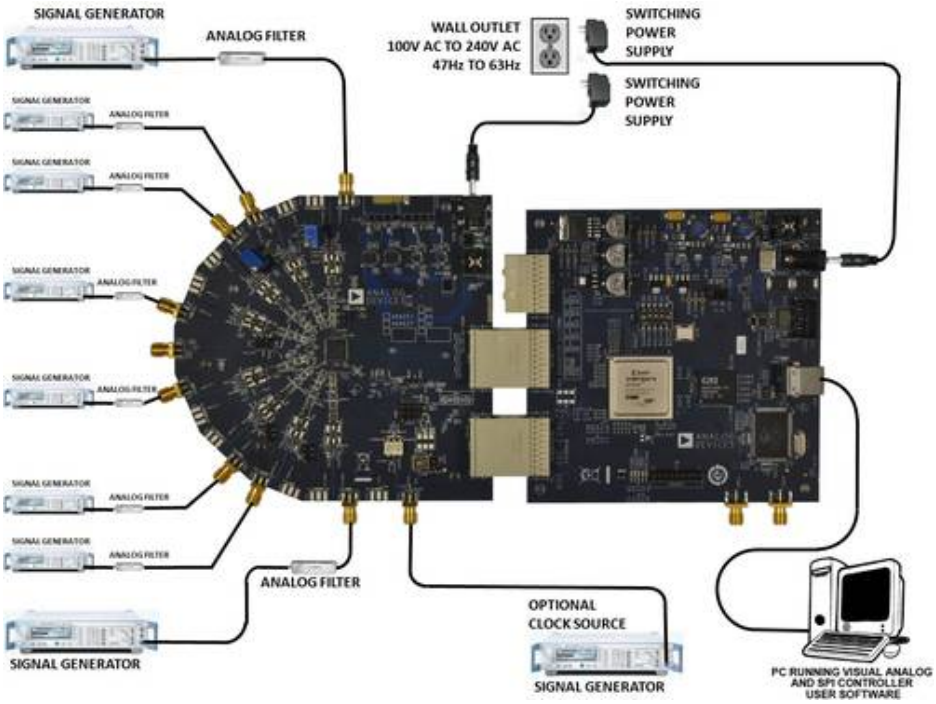

Figure 2. Schematic of a typical measurement setup for the AD9257-EP using the AD9257-65EBZ evaluation card and HSC-ADC-EVALCZ controller board.

B. Irradiation procedure

We applied both a DC and an AC (e.g. sinusoidal and/or triangle) waveform as the input signal. The sampling frequency was set at 40 Msps. We also evaluated the output sensitivity at different voltage and frequency levels, as shown in the test conditions described below.

A complete set of test conditions were satisfied (e.g. different frequencies, input waveforms, voltage levels) before changing the angle or ion. The flux was maintained low enough to avoid multiple simultaneous ion strikes which can lead to compound effects or bus contention. Beam dosimetry information was recorded for each run, including the beam energy, ion specie, ion energy, ion range in silicon, LET at Bragg peak, fluence, flux, and exposure time. Total ionizing dose from the heavy ion irradiation was calculated from the LET and fluence.

Figure 3 shows a photograph of a decapsulated test sample. Figure 4 shows a photograph of the test setup inside the vacuum chamber at LBNL.

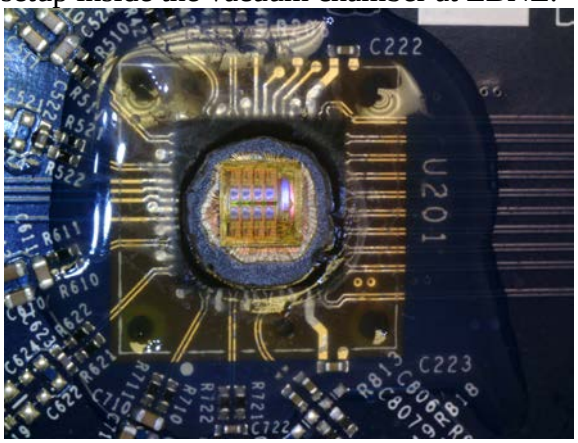

Figure 3. An acid-etched device with exposed die.

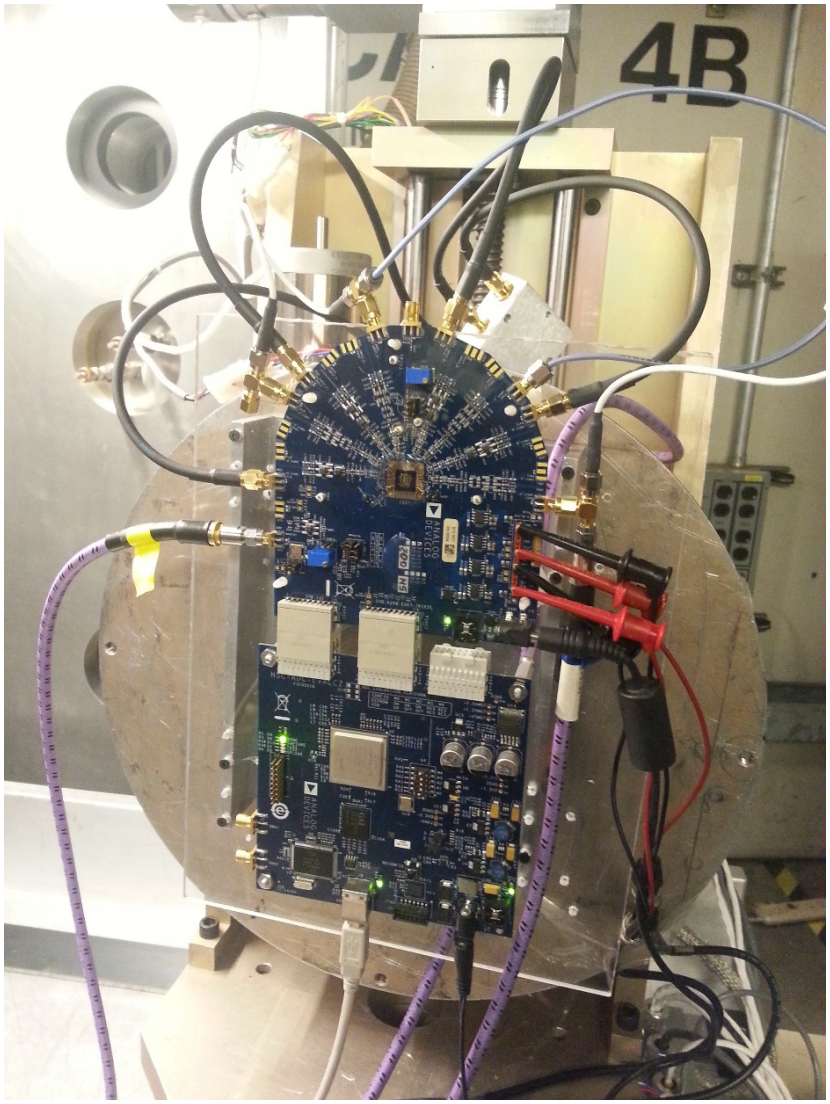

Figure 4. Test setup at LBNL.

i. Single-event upset

During single-event upset characterization, we monitored one channel at a time for each irradiation run. We examined multiple channels (up to 8 per device) to determine any variability in the SEU response.

For a sinusoidal input, the output is bounded with a trigger which envelopes the waveform. The magnitude of the envelope will be determined by the noise margin at the facility.

Following each run, the signal processing program filtered the data log recorded by the VisualAnalog capture program, and saved the events that correspond to SEUs. A list of the irradiation procedure is as follows.

1. Set up DUT (start with SN #6 and #2) in vacuum chamber. Position board to ensure that the stage has full movement capability. Ensure proper functionality of DUT

2. Note the effect of background noise on the signal integrity. Set trigger level slightly higher than the noise level to avoid false triggering
3. Close vacuum chamber, and pump down vacuum
4. Close the irradiation cave
5. Once again ensure functionality including DUT temperature
6. Select appropriate ion specie
7. Set run conditions including the fluence and flux
8. Begin deep capture program and start irradiation
9. Irradiation can be stopped once adequate number of SEU (typically $\geq$ 100 events) is captured or up to a fluence of approximately 1×10^6 cm^{-2} to 2×10^6 cm^{-2} for statistical confidence
10. Following a run, the post processing program will filter and save the output waveforms that correspond to the SEUs (i.e. waveforms that deviated from the trigger)
11. Change the device operating condition (i.e. frequency/sample rate, voltage level, output channel, etc.), and repeat irradiation
12. Change the beam characteristics and repeat irradiation for each set of device operating condition
13. Map out a cross section vs. LET plot

ii. Single-event latchup

For single-event latchup evaluation, each DUT was irradiated to a maximum fluence as time allowed up to a fluence of 1×10^7 cm^{-2} at room temperature. As will be shown, SEFI dominated the SEE response. So several runs were required to accumulate the fluence for a given beam condition. The supply current was monitored *in-situ* during the irradiation. An exponential increase in the supply current can potentially signal the onset of SEL. In the event of a SEL, the procedures were as follows.

1. Shut off the beam immediately, and record the fluence
2. If the current is in a stable state, allow the DUT to dwell in the latched condition for at least 5 minutes
3. Attempt to recover operation by first reset then power cycle
4. After the device recovers functionality, the operator should perform parametric characterization to examine for degradation (i.e. ENOB calculation, current levels, etc.)
5. If the part shows no degradation, then irradiation can continue
6. Determine the SEL LET threshold, and map out a cross section

C. Test Conditions

Test Temperature:	Ambient temperature
Operating Frequency:	40 Msps (for DC and AC input defined below)
Input Voltage (DC):	0.050 V, 0.95 V, 1.3 V, and 1.7 V
Input Voltage (AC):	0.050 V_{pp} at 15MHz
Supply Voltage:	1.8 V_{pp}
Angles of Incidence:	0^o (normal) to 60^o (or maximum allowable)

Parameters: 1) Output voltage
2) Supply current
3) Supply voltage
4) Test Pattern/Delta Counts

VI. Results

A. Single-event functional interrupt

We found that SEFI dominated the SEE response during heavy ion testing. SEFI occurred with both DC and AC modes. The SEFI characteristics can be generally categorized as following:

1. Significant increase in noise (> 100 mV_{pp})
2. Output is stuck at supply rail.
3. Output drops out.

The supply currents either remained stable during a SEFI, or the analog supply may drop out in some events. The majority of SEFIs required power cycle to recover normal functionality. Figure 5 shows the SEFI cross section as a function of effective LET. The SEFI LET threshold is between 1.8 and 3.5 $MeV \cdot cm^2/mg$. Table III shows the Weibull fit parameters at 50% and 95% confidence level (CL). Table IV shows the SEFI rates for background galactic cosmic ray (GCR) and a large solar event for the PACE orbit with 1000 mils equivalent Al shielding.

The worst-case event rate in the second row of the table represents the rate from the worst week of a solar event with the same magnitude as that of the October 1989 solar event. In the more likely scenario that the satellite encounters smaller magnitude solar flares, the upset rate should be adjusted accordingly. Therefore, we also calculated the solar event rate for each solar active year using a probabilistic model [2]. So, the event rate shown in the last row of table IV can be adjusted according to the number of solar active years in a mission.

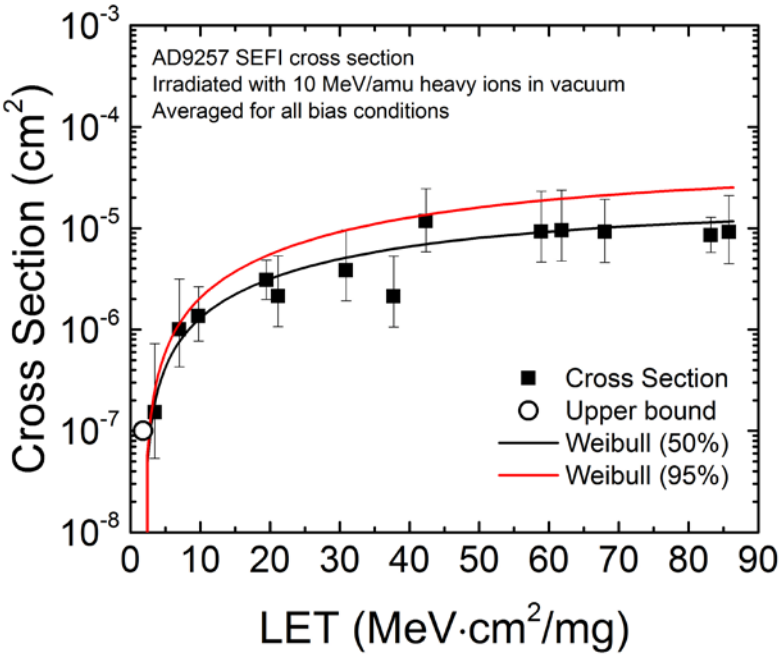

Figure 5. SEFI cross section vs. LET for the AD9257 irradiated with 10 MeV/amu heavy ions in vacuum.

Table III
SEFI cross section Weibull parameters for 50% and 95% CL.

Parameter	50% CL	95% CL	Unit
LET_0	1.9	1.9	MeV·cm²/mg
Sigma	1.50E-05	3.50E-05	cm²
Exponent	1.2	1.3	*NA*
Width	60	70	MeV·cm²/mg

Table IV
SEFI event rate at 50% and 95% CL for background GCR and solar event. The solar flare rate is further given by events per active year using a probabilistic model [2].

Environment 1000 mils Al	50% CL	95% CL	Unit
Background GCR	1.84×10^{-3}	2.98×10^{-3}	Per device-year
Solar event	6.85×10^{-5}	1.15×10^{-4}	Per device-week
Solar flare rate scaled by event per active year [2]	2.40×10^{-6}	4.03×10^{-6}	Per device-year

B. Single-event upset

In addition to SEFI, the part is also susceptible to SEU. Post-irradiation processing of the data sets extracted the SEUs from the background data. The events varied in length and magnitude. Figure 6 shows a plot of the amplitude and duration of all SEUs classified by LET. The SEU characteristics in the plot were determined with a trigger level of ±50 mV. A trigger of ±30 mV produced similar SEU counts, with some of the same SEUs lengthened in duration due to the smaller trigger size. The majority of the SEUs had relatively large voltage amplitudes. Also, high LET ions produced SEUs with longer durations (>100 samples). Figures 7 − 9 shows examples of SEUs.

Figure 10 shows the SEU cross section as a function of effective LET. We observed a SEU LET threshold down to 3.5 MeV·cm^2/mg. We note that the fluence for each run was relatively low, due to the time required for data transfer from the test board to the user PC. So, a SEU was not be observed and captured if it occurred during that dead time. The effective fluence in the cross section also take into account this dead time, leading to the scatter in the dataset. We also assumed a LET threshold of 1 MeV·cm^2/mg for the Weibull fit for conservatism.

Table V shows the Weibull parameters at 50% and 95% confidence level (CL). Table VI shows the SEU event rates from background galactic cosmic ray and solar event for the PACE mission behind an equivalent of 1000 mils spherical Al shielding. The last row shows the scaled solar flare rate by solar active year.

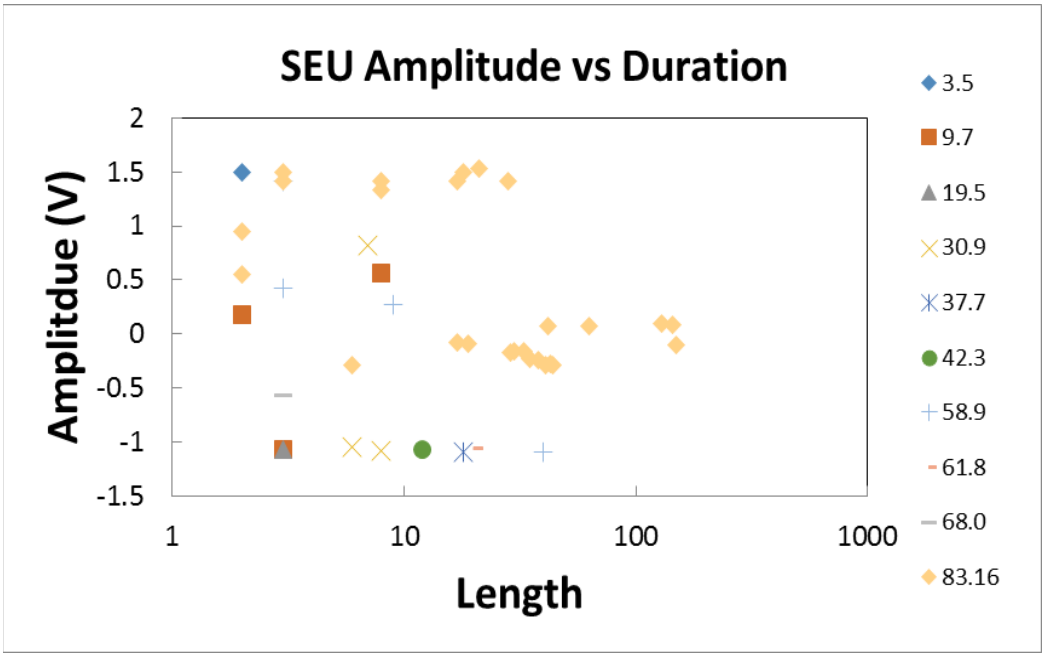

Figure 6. SEU amplitude vs. sample length for the AD9257 irradiated with 10 MeV/amu heavy ions in vaccum. Effective LET values have units of MeV·cm^2/mg. Sampling frequency is 40 Msps. DC input varied from 0.050 to 1.70 V. The trigger level was set at ±50 mV for processing the SEU.

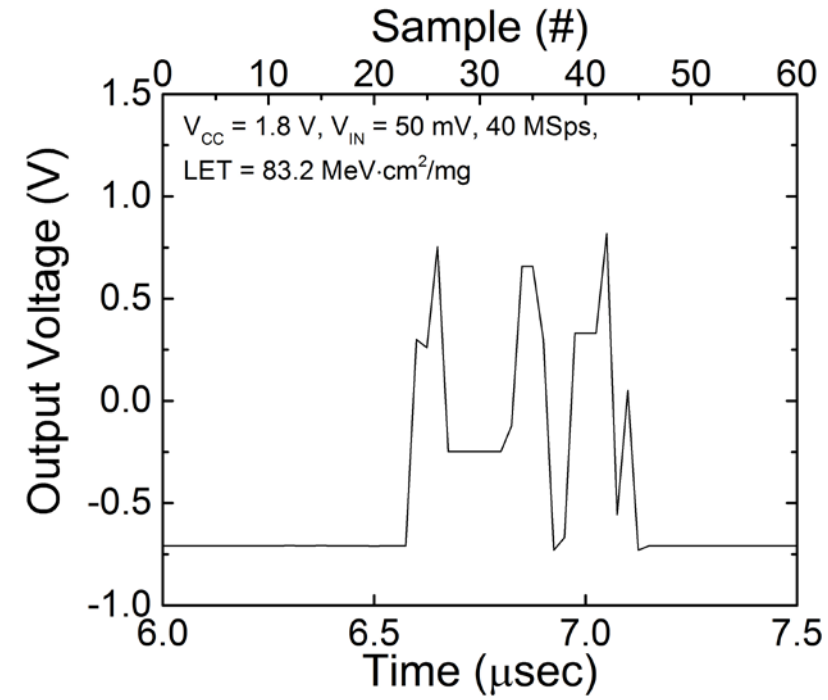

Figure 7. Output voltage vs. time or sample length for a SEU.

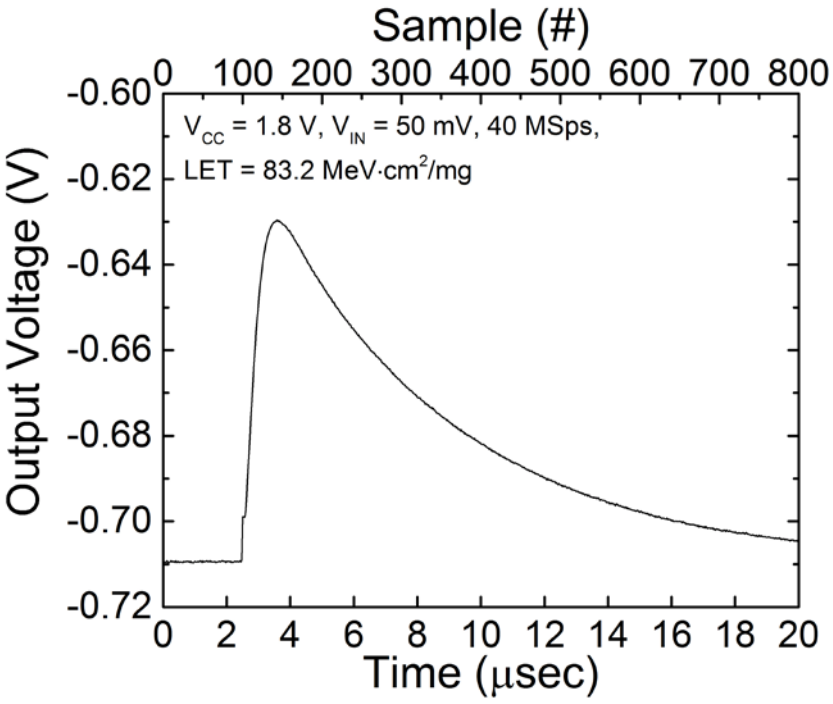

Figure 8. Output voltage vs. time or sample length for a SEU.

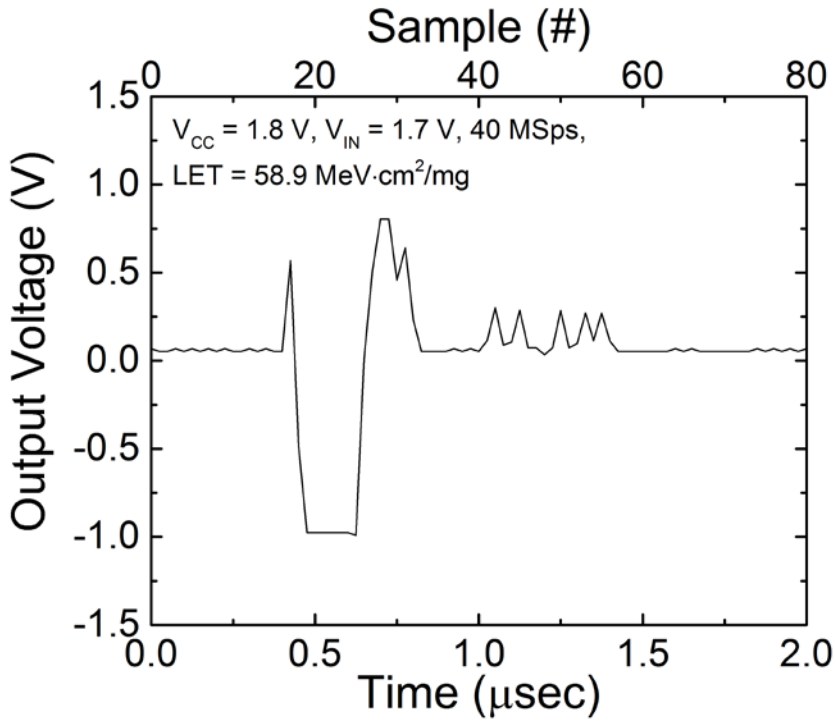

Figure 9. Output voltage vs. time or sample length for a SEU.

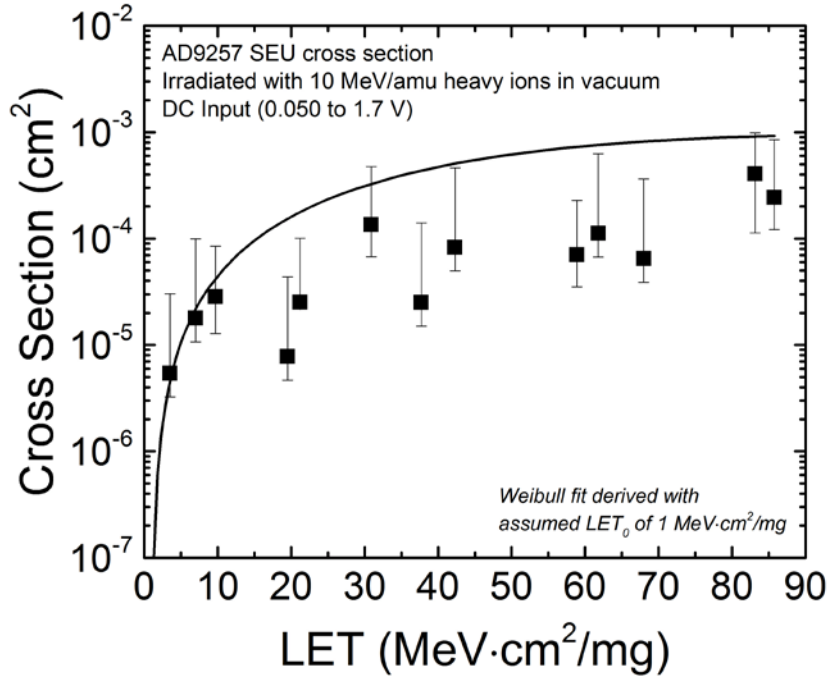

Figure 10. SEU cross section vs. LET for the AD9257 irradiated with 10 MeV/amu heavy ions in vacuum. Sampling frequency is 40 Msps. DC input varied from 0.05 to 1.7 V. We assumed a LET threshold of 1 MeV·cm²/mg for the Weibull fit.

Table V
SEU cross section Weibull fit parameters at 95% CL.

Parameter	95% CL	Unit
LET_0	1	MeV·cm^2/mg
Sigma	1.50 ×10^{-3}	cm^2
Exponent	1.8	*NA*
Width	50	MeV·cm^2/mg

Table VI
SEU event rate at 95% CL for background GCR and solar event. The solar flare rate is further given by events per active year using a probabilistic model [2].

Environment 1000 mils Al	95% CL	Unit
Background GCR	8.02 × 10^{-2}	Per device-year
Solar event	3.30 × 10^{-3}	Per device-week
Solar flare rate scaled by event per active year [2]	1.16 × 10^{-4}	Per device-year

C. Single-event latchup

The part did not exhibit SEL under normal operating conditions up to a LET of 85.8 MeV·cm^2/mg. The supply voltages were biased at 1.8 V. Figure 11 shows the upper bound SEL cross section. The open symbols represent the cross section for 1 event (1/fluence), which is the 63% CL upper bound for observing 0 event in a Poisson process. The upper error bars represent the upper bound at 95% CL. Table VII shows the Weibull fit parameters. The cumulative fluence is 1 × 10^7 cm^{-2} at a LET of 10 MeV·cm^2/mg. So we assumed a LET_0 of 10 MeV·cm^2/mg for the Weibull fits. Using these Weibull parameters, we determined the upper bound for the SEL rates, as shown in Table VIII.

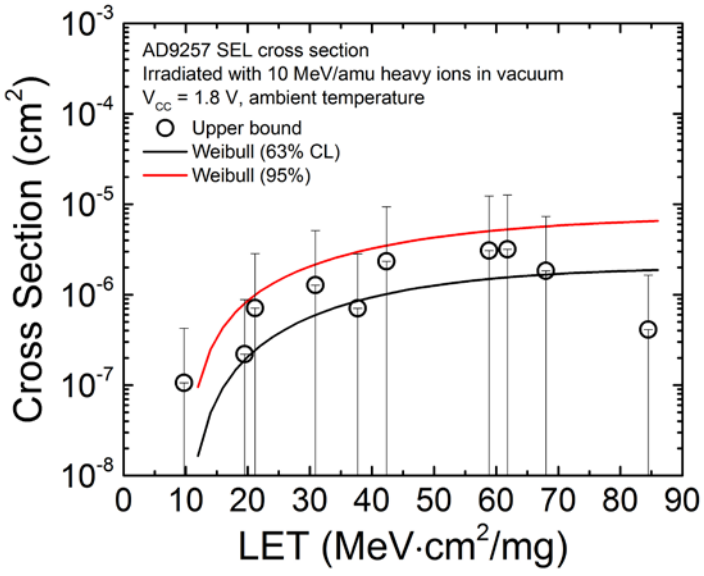

Figure 11. SEL upper bound cross section vs. LET for the AD9257 irradiated with 10 MeV/amu heavy ions in vacuum at ambient temperature.

Table VII
SEL upper bound cross section Weibull fit parameters at 63% and 95% CL.

Parameter	63% CL	95% CL	Unit
LET_0	10	10	MeV·cm^2/mg
Sigma	2.00×10^{-6}	7.5×10^{-6}	cm^2
Exponent	1.6	1.4	*NA*
Width	40	45	MeV·cm^2/mg

Table VIII
SEL upper bound rate at 63% and 95% CL for background GCR and solar event. The solar flare rate is further given by events per active year using a probabilistic model [2].

Environment 1000 mils Al	63% CL	95% CL	Unit
Background GCR	3.24×10^{-5}	1.79×10^{-4}	Per device-year
Solar event	1.77×10^{-6}	8.07×10^{-6}	Per device-week
Solar flare rate scaled by event per active year [2]	6.20×10^{-8}	2.82×10^{-7}	Per device-year

In addition, we irradiated the part biased with only supply voltages active, and no input signal. We carried out irradiation at an effective LET of 68 and 85.8 MeV·cm^2/mg with the bias only condition, and observed SEL in both cases. Figure 12 shows the SEL cross sections for those two events together with the upper bound cross sections under normal device operating conditions. Figure 13 and 14 show the supply current characteristics for each SEL. For the SEL in Figure 13, the supply was clamped at about 0.225 A. The supply was not clamped for the SEL in Figure 14. The digital supply also dropped out upon SEL for the second event in Figure 14. In the second case, we allowed the irradiation run to continue after observing SEL. The current eventually stabilized to about 0.68 A. In both cases, a power cycle recovered functionality. The supply current returned to nominal levels as prior to SEL.

We subsequently carried out a 1000 hour life test on the part that exhibited SEL in Figure 14. The part was biased at nominal supply level (1.8 V). The temperature was set at 125ºC. We periodically extracted the part and checked for functionality. The test sample remained functional throughout and following the 1000 hour life test, with no signs of parametric degradation. The supply current remained unchanged from the start of the life test. This suggests that the SEL was not destructive and did not cause latent damage to the device. The fact that the part did not show SEL under normal operating conditions, but exhibited SEL with bias only further suggests a difference in the SEL susceptibility for the different operating states. The results indicate that the part has reduced sensitivity to SEL under normal operating conditions.

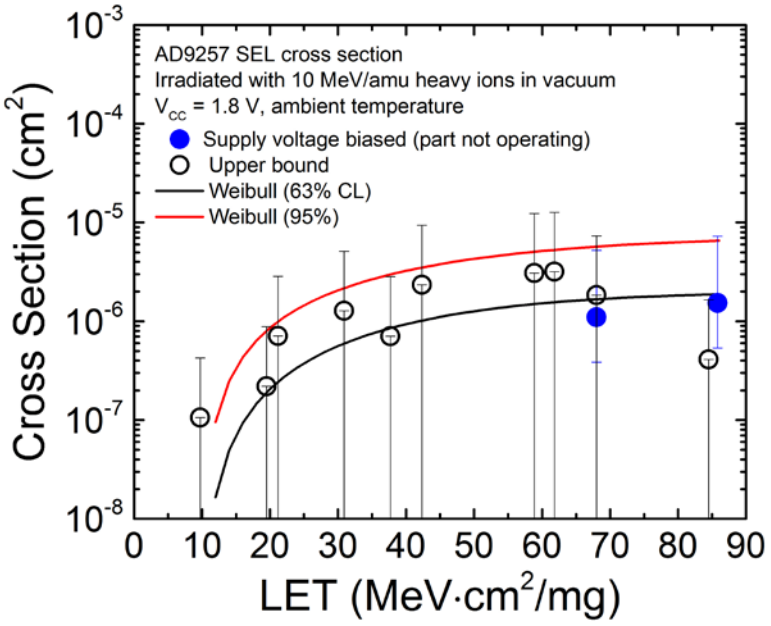

Figure 12. SEL upper bound cross section vs. LET for the AD9257 irradiated with 10 MeV/amu heavy ions in vacuum at ambient temperature. SEL cross sections for the supply bias only condition is shown in solid blue symbols.

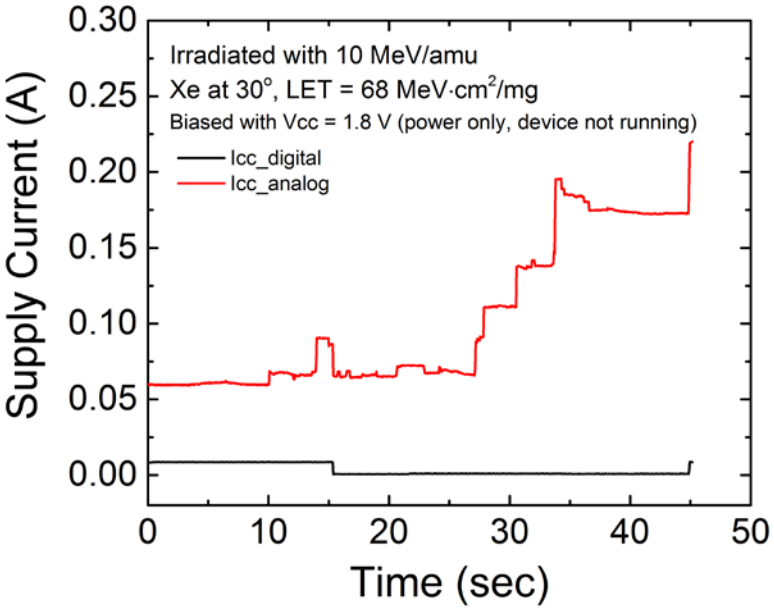

Figure 13. SEL current characteristics for the AD9257 irradiated with Xe at 30°. The part was biased at the supply voltages only and not operating. The supply currents were clamped at approximately 225 mA.

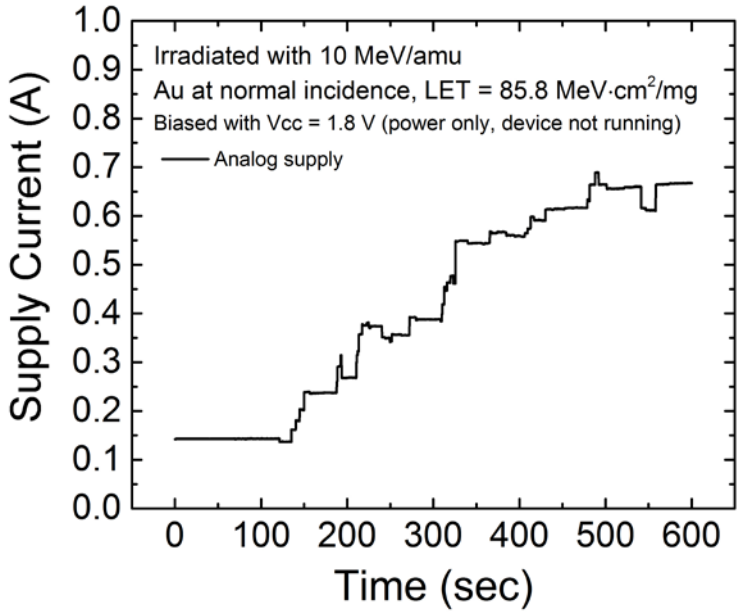

Figure 14. SEL current characteristics for the AD9257 irradiated with Au at normal incidence. The part was biased at the supply voltages only and not operating. There is no current limiting mechanism in place.

VII. Reference

[1] Analog Devices, Inc. (2013, April), "*AD9257: Octal, 14-Bit, 40/65 MSPS Serial LVDS 1.8 V A/D Converter (Rev. A)*" [Online]. Available: http://www.analog.com/media/en/technical-documentation/data-sheets/AD9257.pdf. Accessed on: May 9, 2016.

[2] M. A. Xapsos, G. P. Summers, J. L. Barth, E. G. Stassinopoulos, and E. A. Burke, "Probability model for worst case solar proton event fluences," *IEEE Trans. Nucl. Sci.*, vol. 46, pp. 1481-1485, Dec. 1999.